

Appendix from S. R. Hall et al., “Variation in Resource Acquisition and Use among Host Clones Creates Key Epidemiological Trade-Offs” (Am. Nat., vol. 176, no. 5, p. 557)

Additional Methods, Empirical Results, and Simulation Results

In this appendix, we provide supplemental information pertaining to the experiments, empirical results, and models described in the main text.

Experiments: Clearance Rate, Our Feeding Rate Metric

We used radiotracer methods to estimate clearance rates of 11 clones. This standard procedure involves labeling algal food with a carbon radioisotope and allowing *Daphnia* to graze on it for a short period. We then compared the amount of radioactive carbon in *Daphnia* to that contained in the algae to make our calculations.

Algae Preparation

Scenedesmus was centrifuged (at 3,000 *g* for 5 min) to remove the carbonate-rich algae growth medium. The resulting pellet was resuspended in a medium with a reduced carbon content to enable maximum uptake of the radiotracer by algae. Algal suspensions were incubated with 20–40 $\mu\text{Ci } ^{14}\text{C-NaCO}_3$ on a magnetic spinner overnight and were thereafter centrifuged to remove the radiotracer still present in the solution. The produced pellet was resuspended in filtered lake water and diluted to 2.0 mg mass L^{-1} .

Daphnia

On each experimental day, 1-, 3-, or 6-d-old *Daphnia* were transferred into 50-mL food suspensions (2.0 mg *Scenedesmus* per L) and allowed to acclimate for >30 min before the start of the experiment. To this suspension, 50 mL of 2.0 mg L^{-1} radiolabeled algae suspension was added, denoting the start of the measurement of clearance rate (i.e., volume of habitat from which food was cleared per unit time, and not immunological clearance of infection). From this 100-mL algal suspension, 2 mL were pipetted onto a filter to allow for measurement of the isotopic activity in the algae in units of disintegrations per minute (DPM). Our feeding metric (clearance rate) was measured over 2–6 min, ensuring that this time was lower than the species-specific gut-passage times (based on C. Becker, unpublished data). Feeding experiments were interrupted by sieving animals through a 153- μm mesh; animals were then rinsed twice in filtered lake water before being transferred into 100 mL of filtered water and then into scintillation vials. Animals were dissolved in 0.5 mL of tissue solubilizer (TS-2, RPI, Mt. Prospect, IL), and ^{14}C activities were determined with 10 mL of toluene scintillation cocktail (High-Flash Safety-Solve, RPI) on a Wallac liquid scintillation counter. Clearance rates (mL per individual per h) were calculated from ^{14}C labeling in *Daphnia* (DPM per individual) divided by time feeding on labeled food divided by labels in algae (DPM mL^{-1}).

After estimating the feeding rate metric for each batch of animals, we fitted linear regression through the size–feeding metric data (fig. A1). This regression then allowed us to estimate the feeding metric of a 1.5-mm-long *Daphnia*, which represents the approximate size that most host animals reached at the start of the infectivity (susceptibility) assays. We bootstrapped 95% confidence intervals around this estimate by randomly drawing data from each of the three size classes, fitting the line, estimating the metric at 1.5 mm, and repeating this process 10,000 times.

Experiments

Infection Rate Assays to Measure Host Susceptibility

Figure A2 presents the actual infection prevalence data. Infection prevalence at lower and higher spore doses correlated quite tightly with infectivity ($R = 0.094$, $P < .001$, and $R = 0.91$, $P < .001$, respectively). Furthermore, infection prevalences at the two spore doses were also strongly and positively related ($R = 0.91$, $P < .001$).

Relationships with Fecundity Scaled Instantaneously and the Feeding Metric–Juvenile Growth Rate Mismatch

We provide a complementary set of results involving fecundity that are scaled instantaneously. Such instantaneous measures provide a better match to the parameters of the ordinary differential equation models used to track the dynamics of disease. We estimated the instantaneous birth rate of uninfected, unexposed hosts (b_s) by equating b_s with instantaneous growth rate (r_s), calculated using the standard Euler equation ($1 = \sum_{l,m_x} \exp(-r_s x)$, where l_x is fecundity and m_x is survivorship to day x ; since almost all unexposed hosts survived through the duration of the experiment, m_x typically equaled or nearly equaled 1.0). Using the same procedure, we estimated the instantaneous growth rate of infected hosts (r_1). Since these animals died from infection, this statistic included both fecundity and survival components. However, it likely reflected mostly variation in fecundity, since r_1 correlated positively with arithmetic birth of infected hosts $R = 0.83$, $P = .002$) while r_1 and time until death were not related at all ($R = 0.01$, $P = .97$). Additionally, we calculated an analogous metric for proportional fecundity, the ratio of instantaneous growth (birth) rates ($r_1 : b_s$). This proportional metric was positively correlated with the one shown in the text ($R = 0.78$, $P = .004$).

The results involving instantaneously scaled reproduction mirrored those produced using arithmetic scaling. We found positive relationships between instantaneous birth rate of uninfected hosts (b_s) and the feeding metric and susceptibility and a negative correlation to time until death (fig. A3). The feeding metric–instantaneous birth rate link (fig. A3) also probably stemmed from a negative correlation between the feeding metric and the age at first reproduction (i.e., hosts that ate faster reproduced at an earlier age: $R = -0.71$, $P = .022$; these clones reproducing earlier had higher instantaneous birth rate [$R = -0.69$, $P = .014$] and higher fecundity [$R = -0.74$, $P = .006$; relationships not shown]). The feeding metric did not correlate significantly with juvenile growth rate (fig. A4). Also, r_1 did not correlate with time until death ($R = 0.07$, $P = .84$), host susceptibility ($R = 0.15$, $P = .66$), or the feeding metric ($R = 0.28$, $P = .44$). Additionally, the correlation between the feeding metric and the proportional fecundity metric, $r_1 : b_s$, was not significant ($R = -0.13$, $P = .71$). However, clones with higher juvenile growth rate also tended to have higher fecundity when infected (fig. A5A, A5B) and higher proportional fecundity (fig. A5C, A5D). As a consequence, spore yield correlated with r_1 and $r_1 : b_s$ (fig. A5E, A5F) but not with birth rate of uninfected hosts ($R = 0.30$, $P = .35$).

The lack of relationship between the feeding rate metric and juvenile growth rate merits some discussion. Juvenile growth rate and instantaneous birth rate ($b_s = r_s$) of uninfected hosts were also not correlated. These results seem surprising, given that juvenile growth rate assays typically correlate strongly with r measured across broad gradients of resource quality and quantity (Lampert and Trubetskova 1996; Tessier et al. 2000; Tessier and Woodruff 2002). The strength of this correlation between juvenile growth rate and r may be weakened by the somewhat narrow ranges of growth rate among host clones. However, clonal variation in other traits that influence growth, such as conversion efficiency, maintenance costs, growth costs, and allocation to growth versus reproduction (Yampolsky and Ebert 1994; Kooijman 2000), do not have to correlate with feeding rate. As far as we know, no one has measured the correlation structure of these physiological traits among *Daphnia* genotypes, so data from the literature cannot tell us whether variation in them might predictably weaken the feeding metric–growth rate link. Whatever the cause here, readers should still appreciate that the juvenile growth rate metric predicts a trade-off.

Dynamic Energy Budget Model

The dynamic energy budget (DEB) model was presented in full detail elsewhere (Hall et al. 2009b). However, we slightly modified some of the parameter values here. To enable cross referencing, we present the parameters used here in table A1. We also present additional simulation results that complement findings in the text. First, we see how the spore yield–fecundity trade-off should arise when clones vary only in the feeding metric (fig.

A6). Spore production per host increases with feeding metric (fig. A6A). Since susceptibility also increases with the feeding metric, the model predicts that there should be a positive relationship between susceptibility and spore yield, but this relationship in the data was only marginally significant (fig. A6B). Also, given the negative feeding rate–survivorship relationship (fig. 2), the model predicts that hosts producing more spores (high feeding metric) should die faster than hosts producing fewer spores (low feeding metric; fig. A6C). Fecundity of uninfected hosts (fig. A6D) should also increase with spore production, a result that is hinted at in the data. Thus, the “control” (uninfected)-fecundity trade-off considered by Miller et al. (2005) readily emerges from the DEB model, assuming that clones vary in feeding rate. The DEB model predicts that these relationships should also emerge, assuming that clones vary in conversion efficiency or maintenance costs (not shown). This means that spore yield–infected fecundity relationships can readily arise even if feeding rate and juvenile growth rate are not tightly connected (fig. A4).

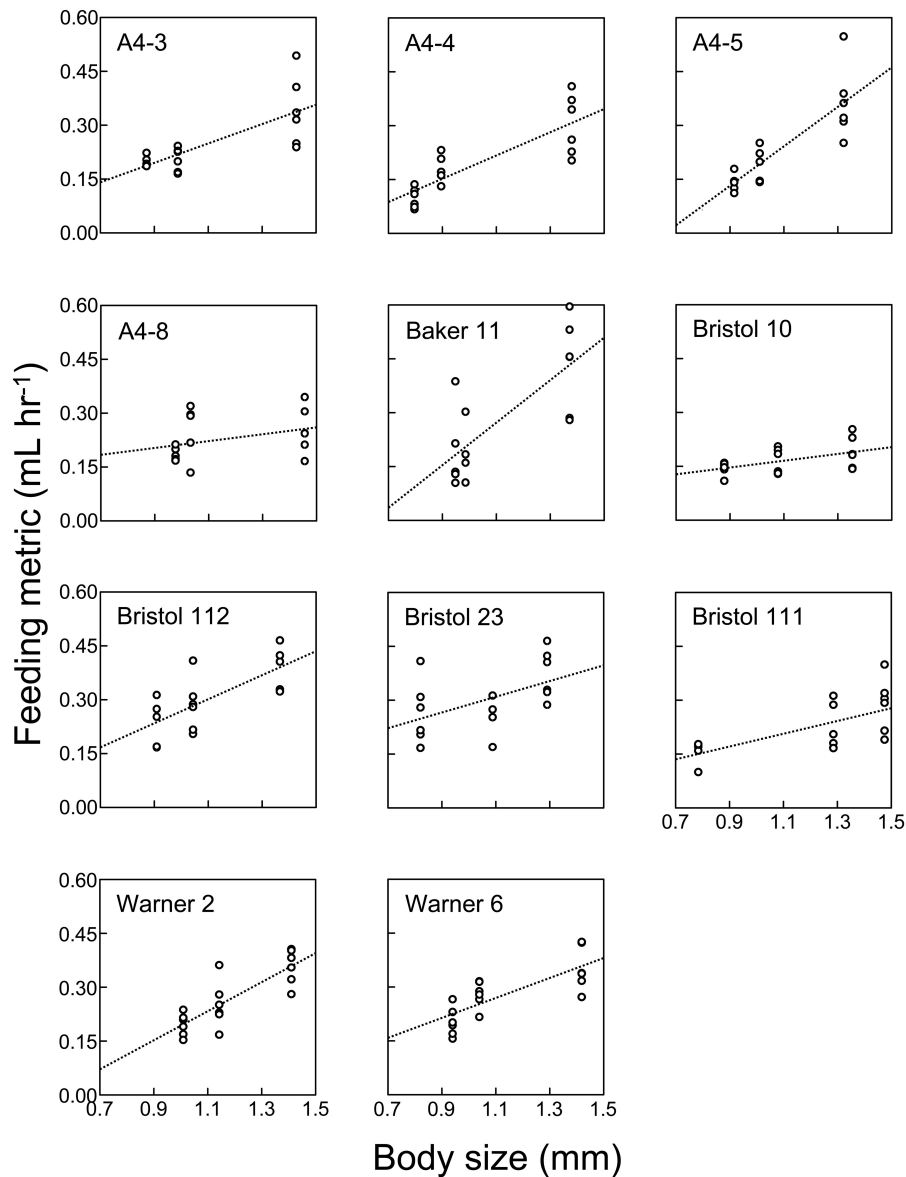


Figure A1: Raw data of the feeding rate metric for 11 of the clones of host *Daphnia dentifera*, scaled in terms of milliliters of water cleared per hour.

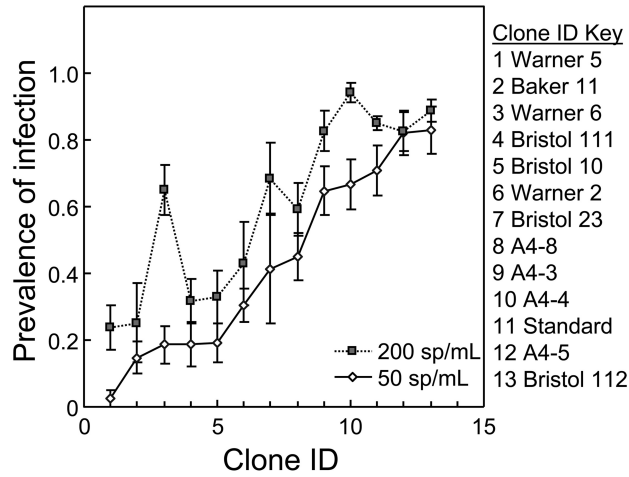


Figure A2: Prevalence (proportion) of infection of each of the 13 *Daphnia dentifera* clones exposed to a lower (50) or higher (200 spores mL⁻¹) dose of the fungal parasite *Metschnikowia bicuspidata*. Clones are sorted from lowest to highest prevalence when exposed to the lower spore dose. Points are means \pm 1 standard error.

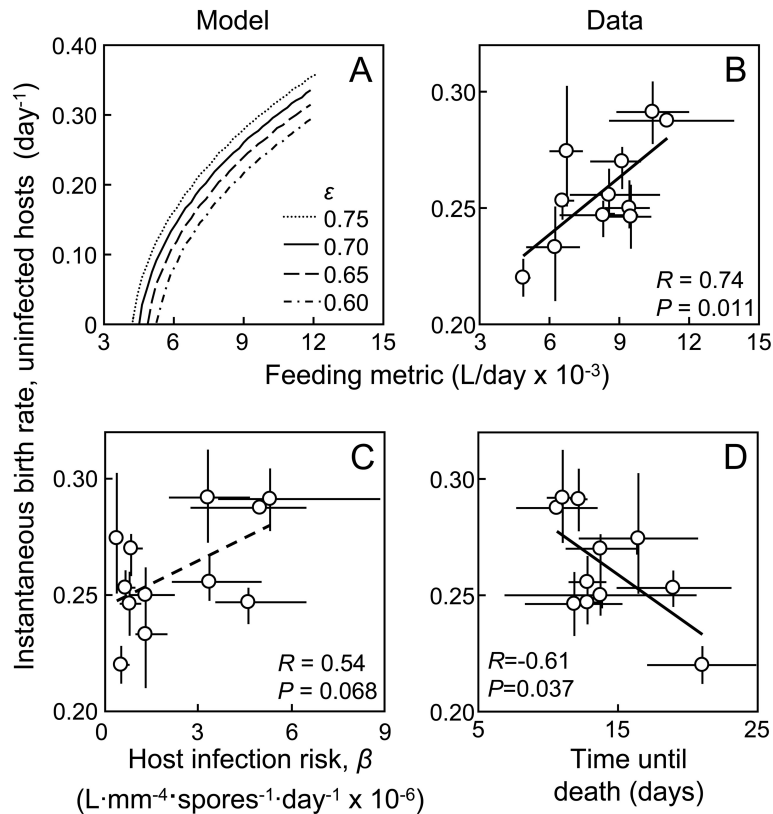


Figure A3: Analog of figures 1 and 2 in the text, showing relationships with fecundity of uninfected hosts scaled instantaneously. *A, B*, Instantaneous fecundity is predicted to increase with the feeding metric in the dynamic energy budget model (*A*) and is observed in the data (*B*). *C, D*, Trade-offs arose between host susceptibility (as scaled by the host infectivity parameter, β ; *C*) and survivorship with instantaneous fecundity (*D*).

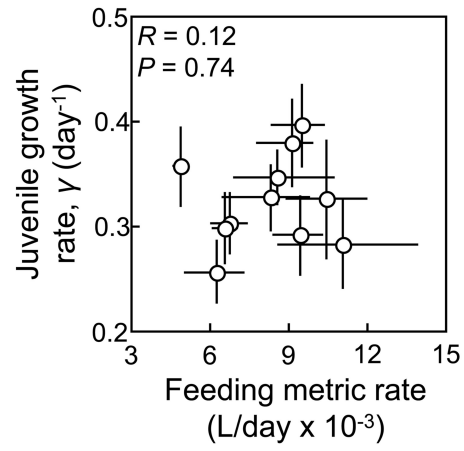


Figure A4: Clonal variation in the juvenile growth rate and the feeding metric were not strongly correlated among hosts. Points are clonal means \pm 95% bootstrapped confidence intervals. Pearson correlation coefficient (R) and P value are also provided.

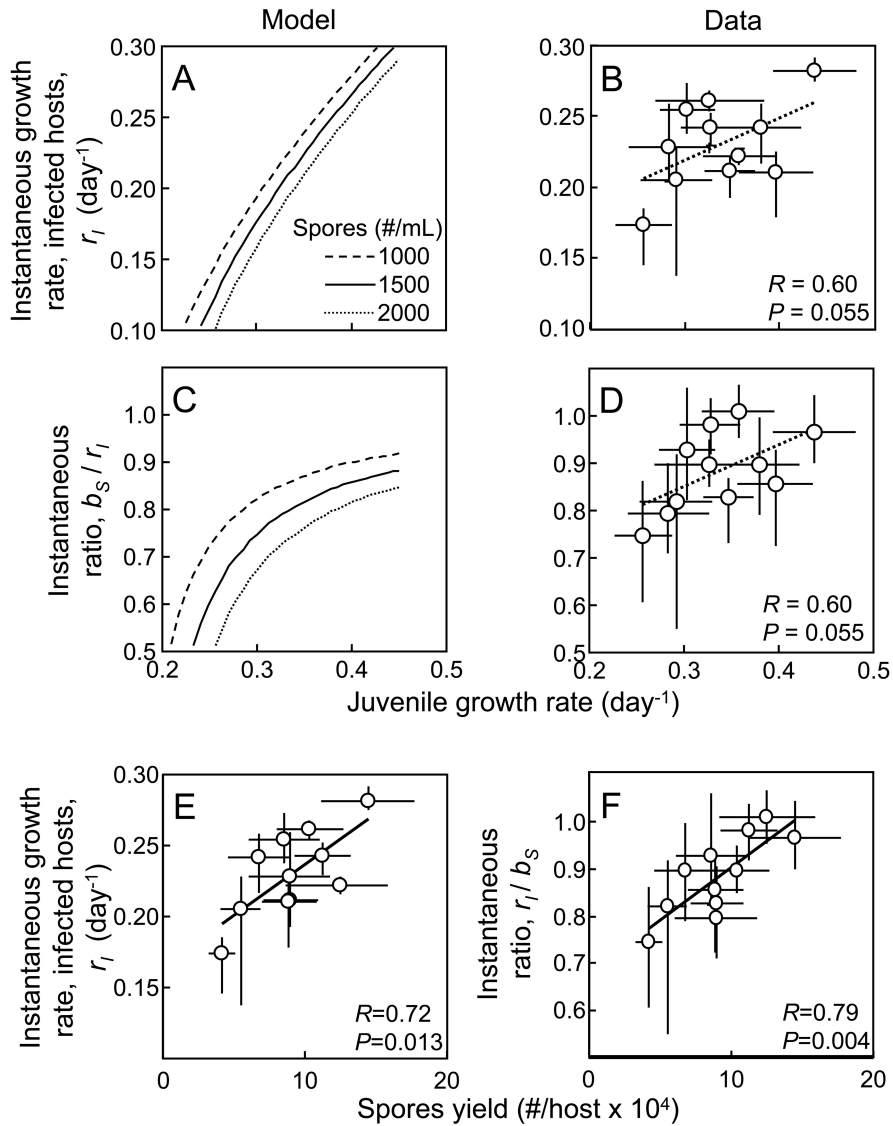


Figure A5: Analog of figures 3 and 4 in the text. *A, B*, The relationship between juvenile growth rate and the instantaneous measure of population growth rate of infected hosts, r_i , emerges in the dynamic energy budget (DEB) model (*A*) and the data (*B*), as does the growth rate–proportional fecundity relationship in the DEB model (*C*) and the data (*D*). *E, F*, The spore yield–infected fecundity trade-off also arises using r_i (*E*) and the proportional fecundity measure r_i/b_s (where b_s is the instantaneous maximal birth rate of uninfected hosts; *F*).

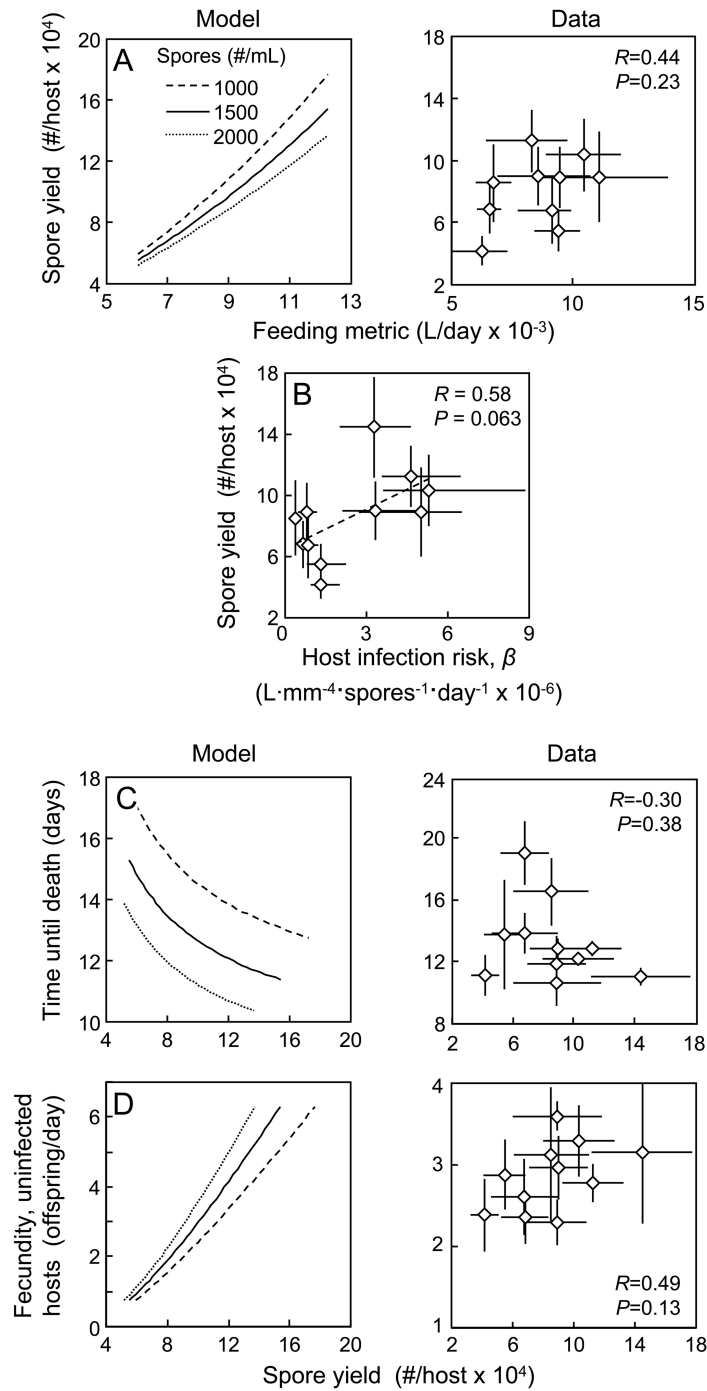


Figure A6: More relationships predicted by the dynamic energy budget model involving spore yield. These predictions are consistent with the data, but all trends are statistically nonsignificant. *A*, Spore yield per host is predicted to increase with the feeding metric. *B*, Spore yield and susceptibility positively correlate (marginally significant). *C*, Survival time when infected and spore yield per infected host correlate negatively. *D*, A trade-off is predicted between spore yield and fecundity. Points are clonal means \pm 95% bootstrapped confidence intervals. Pearson correlation coefficients (R) and P values are also provided.

Table A1

Variables, key fluxes, and parameter values and ranges of parameters used in simulations in the text and appendix A

| Term | Units | Definition | Value or range |
|------------------|---|---|-------------------------------|
| State variables: | | | |
| e | . . . | Reserve energy density (= E/W) | . . . |
| E | mg C | Reserve energy mass (= eW) | . . . |
| N | mg C | Mass of the parasite | . . . |
| R | Number of offspring | Reproduction (offspring) | . . . |
| t | days | Time | . . . |
| W | mg C | Structural mass (weight) of the host | . . . |
| X | mg C L ⁻¹ | Food (algae) | . . . |
| Fluxes: | | | |
| A | mg C day ⁻¹ | Assimilation rate | . . . |
| C | mg C day ⁻¹ | Energy utilization (catabolism) rate | . . . |
| Parameters: | | | |
| a | mg C mm ⁻² day ⁻¹ | Surface area-specific maximal assimilation rate, ef | 4.6×10^{-3} |
| a_N | day ⁻¹ | Maximal assimilation rate, parasite, $\epsilon_N f_N$ | .6 |
| d_N | day ⁻¹ | Combined loss rate, parasite | .08 |
| E_0 | mg C | Carbon investment per offspring | .0021 |
| e_M | . . . | Maximal energy density | 1.0 |
| f | mg C L ⁻¹ mm ⁻² day ⁻¹ | Surface area-specific maximal feeding rate | .009 ^a (.0045–.01) |
| f_N | day ⁻¹ | Maximal feeding rate, parasite | .75 |
| g | . . . | Mass-specific cost of growth | .8 |
| h | mg C L ⁻¹ | Half-saturation constant, host | .1 |
| h_N | mg C | Half-saturation constant, parasite | .005 |
| L | mm | Size of host; relation to W : $W = \alpha L^3$ | . . . |
| L_0 | mm | Initial size of hosts when exposed to parasite | 1.2 |
| m | day ⁻¹ | W -specific maintenance rate, host | .2 ^b (.05–.4) |
| m_N | day ⁻¹ | Loss rate of the parasite | .08 |
| $N_{0,E}$ | mg C | Initial spore mass in beaker to which hosts are exposed | .09, .13, .17 ^c |
| q | . . . | Metabolic cost of production of an offspring | .9 |
| T | days | Interval of food replenishment | 1.0 |
| W_P | mg C | Mass at puberty | .002 |
| α | mg C mm ⁻³ | Conversion for structural mass-length regression | 1.8×10^{-3} |
| ϵ | . . . | Maximal conversion efficiency, host | .75 ^b (.4–.8) |
| ϵ_N | . . . | Maximal conversion efficiency, parasite | .8 |
| κ | . . . | Fraction of energy spent on growth | .2 |
| ρ | . . . | Mechanical threshold of infected host | 1.68 |

Note: Symbols in this table correspond directly to those in Hall et al. (2009b), where the dynamic energy budget model is presented in detail.

^a Range used to produce variation in the feeding rate metric.

^b Default used in all figures.

^c Masses produced from initial spore doses of 1,000, 1,500, and 2,000 spores per mL, respectively, assuming 174 pg per spore (Hall et al. 2009b). Mass of ingested parasite (N_0 of Hall et al. 2009b) is then calculated for a 1.2-mm-long animal as a function of the feeding-rate metric.

Literature Cited Only in the Appendix

- Kooijman, S. A. L. M. 2000. Dynamic energy and mass budgets in biological systems. Cambridge University Press, Cambridge.
- Tessier, A. J., M. A. Leibold, and J. Tsao. 2000. A fundamental tradeoff in resource exploitation by *Daphnia* and consequences to plankton communities. *Ecology* 81:826–841.